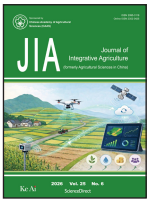
Journal of Integrative Agriculture 2026, 25(6): 2545–2555

Available online at ScienceDirect

Journal of Integrative Agriculture



RESEARCH ARTICLE

Stabilization of plant-derived carbon from different green manure species mediated by carbon-decomposition genes

Tingyu Li[1*], Wei Feng[2*], Tianshu Wang[1], Yili Meng[1#], Shuihong Yao[1#], Xinhua Peng[1]

[1] *State Key Laboratory of Efficient Utilization of Arable Land in China, Institute of Agricultural Resources and Regional Planning, Chinese Academy of Agricultural Sciences, Beijing 100081, China*

[2] *Institute of Agricultural Resources and Environment, Hebei Academy of Agricultural and Forestry Sciences, Shijiazhuang 050051, China*

Highlights

- Green manure application significantly enhances soil organic carbon (SOC) content in both topsoil and subsoil.
- Rapeseed demonstrates a superior capacity to enhance recalcitrant organic carbon (ROC) across the entire soil profile compared to other green manure (GM) types.
- Rye increases carbon functional gene abundance in surface soil, whereas rapeseed and vetch promote it in subsoil.

Abstract

The integration of green manure (GM) crops into traditional cropping systems has regained attention for its potential to improve soil organic carbon (SOC) content in an environmentally sustainable way. However, the effects of carbon (C) input from different GM species on the SOC accumulation and recalcitrant C fractions across soil profile remain inadequately understood. This three-year field study in the North China Plain assessed SOC changes and C fractions of easily oxidizable carbon (EOC) and recalcitrant organic carbon (ROC) in fallow, rye, rapeseed, and vetch systems, with $\delta^{13}C$ analysis for GM-derived C fraction and microbial C-decomposition functional genes. Our results showed that SOC was significantly increased by GMs. Rapeseed was the only species that improved SOC at 20–40 cm, the rapeseed-derived C contributed 2.48% of the SOC. Rye enhanced EOC and ROC at topsoil, rapeseed increased ROC at 20–60 cm, and vetch increased EOC at 40–60 cm. At the topsoil, the abundances of cellulose- and pectin-decomposition genes were increased in vetch and decreased in rye. At 20–40 cm, the pectin- and lignin-decomposition genes were markedly improved by rapeseed, while at 40–60 cm, the chitin-decomposition gene was increased in vetch, indicating the microbial promoting effects by deep roots of vetch and rapeseed. Our results suggest GM species influence SOC deposition depth and the recalcitrance of SOC decomposition, thereby affecting the distribution of SOC accumulation through microbial-driven C decomposition activities.

Keywords: green manure, SOC storage, C recalcitrance, C functional genes

1. Introduction

Soil is the largest global pool of organic carbon (C) in terrestrial ecosystem (Tian *et al.* 2015; Cotrufo and Lavallee 2022). Increasing soil organic carbon (SOC) sequestration in farmland is considered a potential way to achieve C neutrality by 2050 (Griscom *et al.* 2017; IPCC 2018). SOC sequestration reflects the net balance between plant-derived C inputs and outputs *via* decomposition and erosion (Regnier *et al.* 2013; Tian *et al.* 2015). Incorporating green manure (GM) crops into traditional cropping systems has regained attention for their environmentally friendly role in enhancing soil fertility and contributing additional C inputs to soil (Blanco-Canqui *et al.* 2015; Ma *et al.* 2021; Gao *et al.* 2023; Liu *et al.* 2024). However, the actual amount of SOC sequestered from GM crops remains uncertain.

SOC sequestration ultimately depends on the transformation of plant-derived C into SOC stock (de Rouw *et al.* 2015; Huang *et al.* 2023). Evaluating the C sequestration potential of

Received 22 April 2025; Received in revised form 8 September 2025; Accepted 27 October 2025; Available online 7 November 2025
[#]Correspondence Yili Meng, Mobile: +86-13550098888, E-mail: mengyili@caas.cn; Shuihong Yao, Mobile: +86-13720057115, E-mail: yaoshuihong@caas.cn
[*] These authors contributed equally to this study.

© 2026 CAAS. Publishing services by Elsevier B.V. on behalf of KeAi Communications Co. Ltd. This is an open access article under the CC BY-NC-ND license (http://creativecommons.org/licenses/by-nc-nd/4.0/). Peer review under responsibility of Editorial Board of *Journal of Integrative Agriculture*.
doi: 10.1016/j.jia.2025.11.005

GM crops requires not only quantifying their biomass C inputs but also assessing the efficiency of C transformation into SOC (Dou *et al.* 2017). This transformation efficiency can be assessed by using the natural ^{13}C abundance difference between soil and plants, as SOC is usually enriched in ^{13}C due to isotopic fractionation during microbial decomposition of plant residues (Balesdent *et al.* 1987; de Rouw *et al.* 2015; Busari *et al.* 2016; Chen *et al.* 2018; Zhang *et al.* 2022). However, the transformation efficiency of GM-derived C into SOC has not been adequately evaluated among GM crops that differ not only in biomass production but also in C component composition (Tejada *et al.* 2008; Qiao *et al.* 2015; He *et al.* 2020), C/N ratio (Wang *et al.* 2020), and particularly in the way soil microbial communities respond to C inputs (Li *et al.* 2024).

Microbial decomposition is the primary driver of SOC transformation (Berendsen *et al.* 2012). Factors such as microbial metabolic activity and selective utilization of C substrates determine the transformation efficiency (Huang *et al.* 2023). GM biomass contains varying C components such as lignin, pectin and cellulose, which impose different levels of recalcitrance to decomposition (Tejada *et al.* 2008; Qiao *et al.* 2015; He *et al.* 2020; Wang *et al.* 2020). Microorganisms selectively utilize these components, with variation in C-decomposition genes indicating functional shifts in microbial decomposition capacity (Zechmeister-Boltenstern *et al.* 2015; Li *et al.* 2024). However, few studies have systematically assessed the link between microbial C-decomposition functions and the transformation efficiency of GM-derived C into SOC.

While the microbial and substrate-mediated processes ultimately influence the SOC transformation, the consequences of long-term C sequestration are reflected in SOC recalcitrance, which can be evaluated by measuring easily oxidizable carbon (EOC) and recalcitrant organic carbon (ROC) fractions (Haynes 2000; Chen *et al.* 2023; Shi *et al.* 2023). EOC, as the active C pools, is sensitive to agricultural management and serves as an indicator of soil C supply (Haynes 2000; Ramírez 2020; Rocci *et al.* 2021), whereas ROC is less responsive to management practices and better reflects long-term soil storage (Chen *et al.* 2019; Liu *et al.* 2022; Shi *et al.* 2023). GM crops have been reported to influence the contents of both EOC and ROC (Blanco-Canqui *et al.* 2015; Ansari 2022). However, the effects of GM crops on SOC fractions and recalcitrance remain insufficiently understood. Recent studies have shown that SOC recalcitrance varies with soil depth (Xiang *et al.* 2022; Shi *et al.* 2023; Wang *et al.* 2025), though it is still unclear whether such depth-dependent patterns are influenced by GM crops.

Root growth pattern is one of the factors regulating the depth of C deposition, as root pathway serve both as channels for C transfer and hotspots for mineralization (Leue *et al.* 2020). Consequently, contrasting architectures, such as taproot and fibrous systems, can drive distinct variations in SOC dynamics (Kumar *et al.* 2018; Engedal *et al.* 2023). However, most studies have focused only on the surface soils, which fails to capture the full extent of C storage, as roots commonly extend deeper than 20 cm (Materechera *et al.* 1992; Qiao *et al.* 2015; Thorup-Kristensen *et al.* 2020; Engedal *et al.* 2023). To fully evaluate the C sequestration potential of different GM crops, it is essential to assess SOC recalcitrance and its cycling across soil profile.

In the North China Plain, the main maize-producing region in China, continuous maize cultivation has resulted in soil fertility reduction (Magdoff and Weil 2004). To alleviate SOC loss, winter GM crops including hairy vetch (*Vicia villosa* Roth), rapeseed (*Brassica napus* L.), rye (*Secale cereale* L.), ryegrass (*Lolium perenne*), orychophragmus (*Orychophragmus violaceus*) have been promoted. These crops differ in biomass inputs, C composition, root growth, and their capacity to recruit soil microorganisms (Hu *et al.* 2024; Wang *et al.* 2024; Li *et al.* 2025). Therefore, to evaluate SOC sequestration potential in the North China Plain, we aim to determine the effects of the typical GM crops on GM plant-derived SOC, recalcitrant SOC fractions, and microbial C-decomposition functional genes across soil profiles. We hypothesized that: 1) GM species would differentially alter SOC content with depth as well as its recalcitrant fractions; 2) the efficiency of converting GM biomass C into SOC would vary among GM species; 3) microbial C-decomposition genes would regulate the transfer efficiency of plant-derived C into SOC.

2. Materials and methods

2.1. Experimental design and sampling

The experimental site is located in Yangerzhuang Town (117°29′E, 38°16′N), Huanghua City, Hebei Province, China, to the west of Bohai Bay. The site has a warm temperate monsoon climate, with a mean annual temperature of 11°C and an average annual precipitation of 545 mm from 2019 to 2022. The monthly average temperature and accumulated precipitation were presented in Appendix A. The soil type is Fluvisol and has a sand loam texture.

Twelve plots were established in October 2019, arranged in a complete randomized design with four treatments in triplicates. The four winter GM treatments included: (1) fallow as a control (CK), (2) rye (*S. cereale* L.), (3) rapeseed (*B. napus* L.), and (4) hairy vetch (*V. villosa* Roth). Each plot measured 56 m^2 (7 m×8 m) and remained unfertilized during the winter GM growth period. In the subsequent summer maize growth period, the plots received 100 kg N ha^{-1}, 105 kg P_2O_5 ha^{-1}, 120 kg K_2O ha^{-1} at the seedling stage in early June, and an additional 150 kg N ha^{-1} at the flare opening stage of maize in late July. The fertilization rates adhered to the typical regional standards for summer maize. All plots were rain-fed and unirrigated.

In May, winter GM plants were harvested, chopped, and incorporated into the soil by using a rotary cultivator. The CK treatment was periodically weeded by hand, leaving bare soil during winter. In May of 2020, 2021, and 2022, the aboveground biomass of GMs from a 2 m^2 quadrat was chopped and weighed. A 1 kg biomass subsample was collected from each plot, and the remaining biomass was returned to the field. The subsamples were oven-dried at 60°C, and weighed to estimate the moisture content and dry biomass yield, and then sent to the laboratory for further

analysis. Additionally, ten whole plants were sampled per plot to measure the belowground and aboveground biomass ratio (Appendix B), which was used to estimate the yield of belowground biomass.

Initial soil samples were collected in October 2019 before planting the GM crops, using soil probe and ring cutter to obtain 0–20 cm topsoil. Soil profile samples were taken in October 2022 before planting the GM crops. In each plot, two undisturbed soil cores to a depth of 0–100 cm were extracted using a stainless-steel cylinder equipped with diesel drill. The soil cores were transported to the laboratory within the cylinder. They were cut into a 20 cm-section, corresponding to the depths of 0–20, 20–40, 40–60 cm, each with a diameter of 5 cm. The soil core sections were prepared for further physicochemical analysis. In addition, a soil profile to a depth of 0–60 cm was excavated in each plot, and soil ring cutter samples were collected in triplicates at the depths of 5, 15, 30 and 50 cm to represent the soils at 0–10, 10–20, 20–40 and 40–60 cm layers, respectively.

2.2. Soil physicochemical properties

The initial soil samples were analyzed for pH, SOC, TN, ammonium (NH_4^+), nitrate (NO_3^-), bulk density, and texture. Soil pH was measured by mixed soil to water at 1:5 (w/v). The SOC and TN were detected using an elemental analyzer (Elementar Vario EL cube, Elementar, Germany). Soil NH_4^+ and NO_3^- were extracted with 2 mol L^{-1} KCl, the NH_4^+ and NO_3^- concentrations were detected using a continuous flow analytical system (Seal Auto Analyzer AA3, Norderstedt, Germany). The ring cutter samples were dried in oven at 105°C for 24 h and weighed to determine bulk density (Nouri *et al.* 2019). Content of clay, silt and sand were determined by using a hydrometer (Hu *et al.* 2024). The physical and chemical properties of the initial soil samples were presented in Appendix C.

SOC storage (Mg ha^{-1}) was calculated following Xia *et al.* (2022):

$$\text{SOC storage}=\frac{\text{SOC}\times\text{BD}\times\text{h}}{100}\times 10$$

where SOC is the soil organic C content of each soil layer (g kg^{-1}), BD is the bulk density of each soil layer (g cm^{-3}), and h is thickness of the corresponding soil layer (cm).

2.3. C contents and ^{13}C isotope abundance of GM biomass and soil

Subsamples from the 20 cm sections of soil cores (0–20, 20–40, 40–60 cm) were collected and air-dried. The air-dried soil samples and the oven-dried plant biomass samples were ground to pass through 0.15 mm sieve, and then the samples were weighed into a tin capsule to analyze for C content and $\delta^{13}C$ values using an elemental analyzer interfaced to an isotope ratio mass spectrometer (Europa ANCAGSL, PDZ Europa, England).

The GM plant biomass C input (Mg ha^{-1}) was calculated as:

$$C_{input}=(B_{above}+B_{below})\times C_{biomass}$$

where B_{above} and B_{below} are the aboveground and belowground dry biomass yields (Mg ha^{-1} yr^{-1}), and $C_{biomass}$ is the C content of GM biomass (%).

The $\delta^{13}C$ values are reported relative to the Pee Dee Belemnite (PDB) standards. The GM-derived C fraction in SOC was calculated from the $\delta^{13}C$ difference between soil and GM plants (Chen *et al.* 2023), following equations:

$$f=\frac{\delta_{sam}-\delta_{CK}}{\delta_{plant}-\delta_{CK}}$$

where δ_{sam} is the $\delta^{13}C$ value of soil samples from each layer under GM treatment, δ_{CK} is the $\delta^{13}C$ value of soil samples from the corresponding layers under follow CK treatment, and δ_{plant} is the $\delta^{13}C$ value of the corresponding GM plant biomass samples.

2.4. Easily oxidizable carbon (EOC) and recalcitrant organic carbon (ROC)

Subsamples from the 20 cm sections of soil cores (0–20, 20–40, 40–60 cm) were collected, air-dried and passed through 0.15 mm sieves. The EOC content was measured using an oxidation method (Blair *et al.* 1995). A soil sample (0.5 g) was reacted with 25 mL of 0.333 mol L^{-1} $KMnO_4$ and shaken at 200 r min^{-1} for 1 h. The suspension was then centrifuged at 2,000 r min^{-1} for 5 min. The supernatant was diluted, and its absorption at 565 nm was measured using a spectrophotometer (UV-3600i, SHIMADZU, Japan). The amount of $KMnO_4$ consumed was calibrated using a standard curve prepared with 0.1–0.5 mol L^{-1} $KMnO_4$ solutions. The ROC was determined by using a high-temperature digestion method (Rovira and Vallejo 2007). A soil sample (1.0 g) was hydrolyzed with 20 mL of 6 mol L^{-1} HCl at 105°C for 18 h. After hydrolysis, the supernatant was discarded. The unhydrolyzed residue was washed with deionized water through repeated centrifugation and decanting. The final residue was dried at 65°C to a constant weight and analyzed for C content using an elemental analyzer (Elementar Vario EL cube, Elementar, Germany). The changes in C content (ΔSOC, ΔEOC and ΔROC) were calculated by subtracting the SOC, EOC and ROC values of the fallow CK from those of the GM treatments. C stocks were calculated from the product of soil bulk weight, SOC content and soil layer thickness (Yan *et al.* 2023). Soil C pool management index (CPMI) was calculated based on the protocol in Blair *et al.* (1995):

$$\text{C pool activity (CPA)}=\frac{\text{EOC}}{\text{SOC}-\text{EOC}}$$

$$\text{C pool activity index (CPAI)}=\frac{\text{CPA}_{sam}}{\text{CPA}_{CK}}$$

$$\text{C pool index (CPI)}=\frac{\text{SOC}_{sam}}{\text{SOC}_{CK}}$$

$$\text{C pool management index (CPMI)}=\text{CPI}\times\text{CPAI}\times 100$$

where CPA_{sam} refers to the CPA of GM treatments, and CPA_{CK} refers to the CPA of fallow CK treatments.

2.5. The abundance of soil microbial C-decomposition functional genes

Subsamples from the 20 cm sections of soil cores (0–20, 20–40 and 40–60 cm) were collected and immediately stored at –80°C until DNA extraction. Total DNA was extracted from

~0.25 g (dry weight) soil using a commercial soil genome DNA extraction kit (DcP336, Tiangen Biochemical Technology (Beijing) Ltd., China), and quality was checked by using 1% agarose gel electrophoresis and NanoDrop (2000) ultra-microspectrophotometer (Thermo Scientific, USA).

Soil bacterial 16S rRNA, fungal ITS, and microbial C-decomposition functional genes (*sga*, *abfA*, *cex*, *chiA*, *pgu*, and *mpn*) were amplified with primers listed in Appendix D. The PCR reaction was performed in 10 μL reaction (1 μL DNA template, 5 μL SYBR® Green Pro *Taq* HS, 0.5 μL forward/reverse primers, 3 μL of dd H_2O) on a QuantStudio™ 6 Flex (Applied Biosystems®, Carlsbad, USA) under the program: initial denaturation at 95°C for 30 s, followed by 40 cycles of 95°C for 5 s and 60°C for 30 s. Template DNA concentration was adjusted in preliminary experiments to yield Ct values of 15–30. Standard plasmids for each gene were constructed with a pGEM-T vector (Promega, USA), serially diluted (10^1–10^8 copy numbers μL^{-1}), and used to generate standard curves. Gene abundances were expressed as copies mg^{-1} soil.

To compare GM crops with winter fallow CK, gene abundance ratios were expressed as $\log_2$(fold change), where a value of 1 indicates a doubling of gene abundance and −1 indicates halving.

$$\log_2(\text{fold change})=\log_2\left(\frac{\text{Gene abundance}_{GM}}{\text{Gene abundance}_{CK}}\right)$$

2.6. Statistical analysis

The analysis of variance (ANOVA) and Pearson correlation were conducted using SPSS 26.0 (SPSS, Chicago, IL, USA). The ANOVA was employed to evaluate the effects of different GM treatments on soil C input, soil C decomposition functional genes abundance, and changes in C fractions. Differences were considered statistically significant at $P<0.05$. All figures were generated using Origin software 2023b. Redundancy analysis (RDA) to explore the relationships between soil C fractions and the C decomposition functional genes abundance, utilizing the "vegan" package in R version 4.1.0.

3. Results

3.1. Green manure biomass yield and C input

The three GM crops produced significantly different amounts of dry biomass, both above- and belowground, and their C content varied among species (Table 1). Rye had the highest aboveground biomass at 7.05 Mg ha^{-1} yr^{-1}, followed by vetch at 4.20 Mg ha^{-1} yr^{-1}, and rapeseed at 3.96 Mg ha^{-1} yr^{-1}. Belowground biomass followed a similar trend, with rye showing significantly higher biomass than both rapeseed and vetch ($P<0.05$). With differences in the above- and belowground C content of the returned biomass, rapeseed contributed the lowest C input, followed by vetch and rye, with significant differences among GM crops ($P<0.05$) (Fig. 1-A).

The $\delta^{13}C$ of the returned biomass varied among the GM crops (Table 1). After three years of biomass return, the soil $\delta^{13}C$ of GM treatments were significantly lower than that of CK at each depth. The soil $\delta^{13}C$ was particularly low at 20–40 cm in the rapeseed treatment (Fig. 1-B). The SOC fractions derived from GMs did not differ among rye, rapeseed and vetch at 0–20 and 40–60 cm, while at 20–40 cm, SOC fractions derived from rapeseed were significantly higher than those from rye and vetch (Fig. 1-C).

3.2. SOC fractions and CPMI along soil profiles

The SOC content within soil profiles varied depending on vegetation types and soil depth (Fig. 2-A). Overall, SOC content was higher in the surface layer than in the subsoil. At the 0–20 cm, the SOC content in the rye and vetch treatments was significantly higher than in the rapeseed and CK treatments. At the 20–40 cm, the rapeseed treatment showed significantly higher SOC content than the rye and vetch treatments ($P<0.05$). At the 40–60 cm, no significant differences in SOC content were observed among the treatments. A similar trend was observed when comparing SOC storage within the soil profiles, considering variations in soil bulk density (Appendix E). Across the 0–60 cm soil profile, all GM treatments showed higher SOC than CK, with the largest increase observed in rye; however, the ΔSOC in rye did not differ significantly from those in rapeseed and vetch. Both rye and vetch showed substantial increases in SOC at the 0–20 cm depth, but exhibited negative ΔSOC at the 20–40 cm. In contrast, rapeseed had the smallest positive ΔSOC at the 0–20 cm, but achieved a significantly larger ΔSOC than the other two GMs at the 20–40 and 40–60 cm ($P<0.05$) (Fig. 2-D).

The soil EOC and ROC contents varied differently from SOC within soil profiles. At the 0–20 and 20–40 cm, soil EOC content was significantly higher in GM treatments than in the CK, especially in the rye treatment. However, at the 40–60 cm, soil EOC did not differ significantly between GM treatments and CK, except in vetch ($P<0.05$) (Fig. 2-B). Rye had significantly higher ΔEOC than rapeseed and vetch at the 0–20 and 20–40 cm ($P<0.05$), but at the 40–60 cm, the ΔEOC in rye showed a negative increase (Fig. 2-E). The soil ROC contents in rapeseed treatment showed a unique pattern within the soil profiles (Fig. 2-C). At the 20–40 and 40–60 cm, the soil ROC content in rapeseed was significantly higher than in the other treatments ($P<0.05$). This pattern was also observed in ΔEOC, where the rapeseed treatment showed the greatest ΔROC in the subsurface soil. Rapeseed's

Table 1 Dry biomass, C and N content, and $\delta^{13}C$ of green manure crops

Green manure	Aboveground (Mg biomass ha^{-1} yr^{-1})	Belowground (Mg biomass ha^{-1} yr^{-1})	C (%)	N (%)	C:N	$\delta^{13}C$ (‰)[1)]
Rye	7.05±0.82 a	3.10±0.36 a	41.31±1.24 b	1.07±0.03 c	38.51±1.68 a	–63.76±0.14 a
Rapeseed	3.96±1.60 b	1.15±0.46 b	40.72±0.63 b	2.39±0.18 b	17.09±1.21 b	–68.46±0.47 b
Vetch	4.20±0.46 b	1.51±0.17 b	43.05±0.32 a	3.61±0.40 a	12.08±1.48 c	–69.06±0.50 b

[1)] $\delta^{13}C$ values are reported relative to the Pee Dee Belemnite standard.
Data are mean±SD ($n=3$). Different letters indicate significant differences among green manure treatments ($P<0.05$).

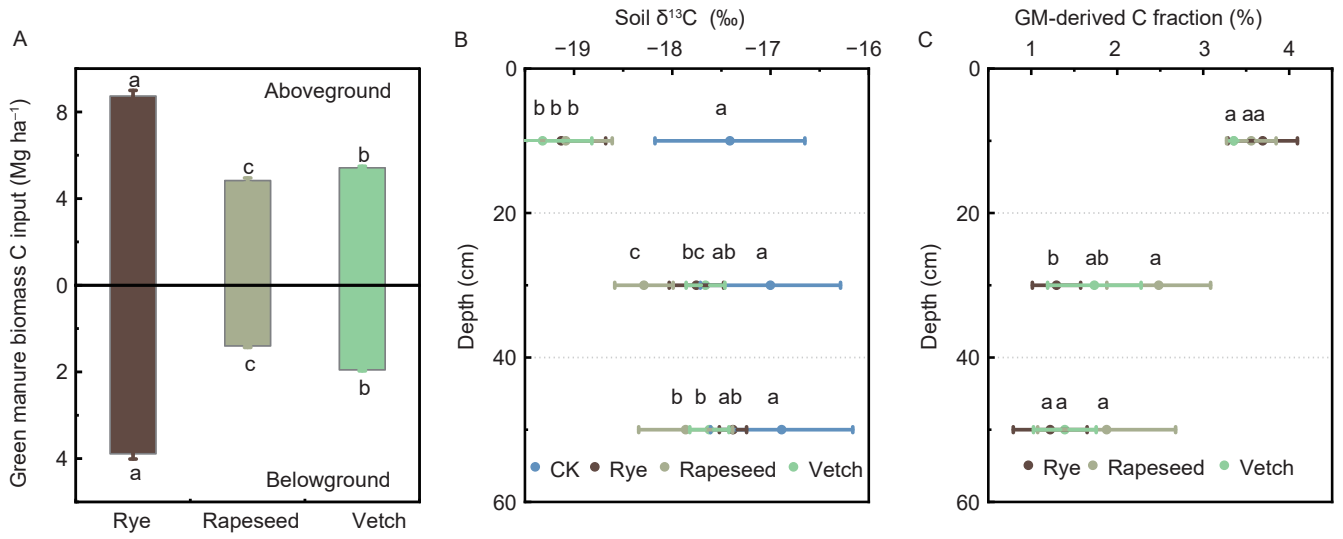


Fig. 1 Green manure C input in three years (A), soil δ¹³C (‰ relative to Pee Dee Belemnite) (B), and green-manure derived C fraction in soil organic carbon (C). Error bar is SD (n=3). Different letters indicate significant differences among green manure treatments (P<0.05).

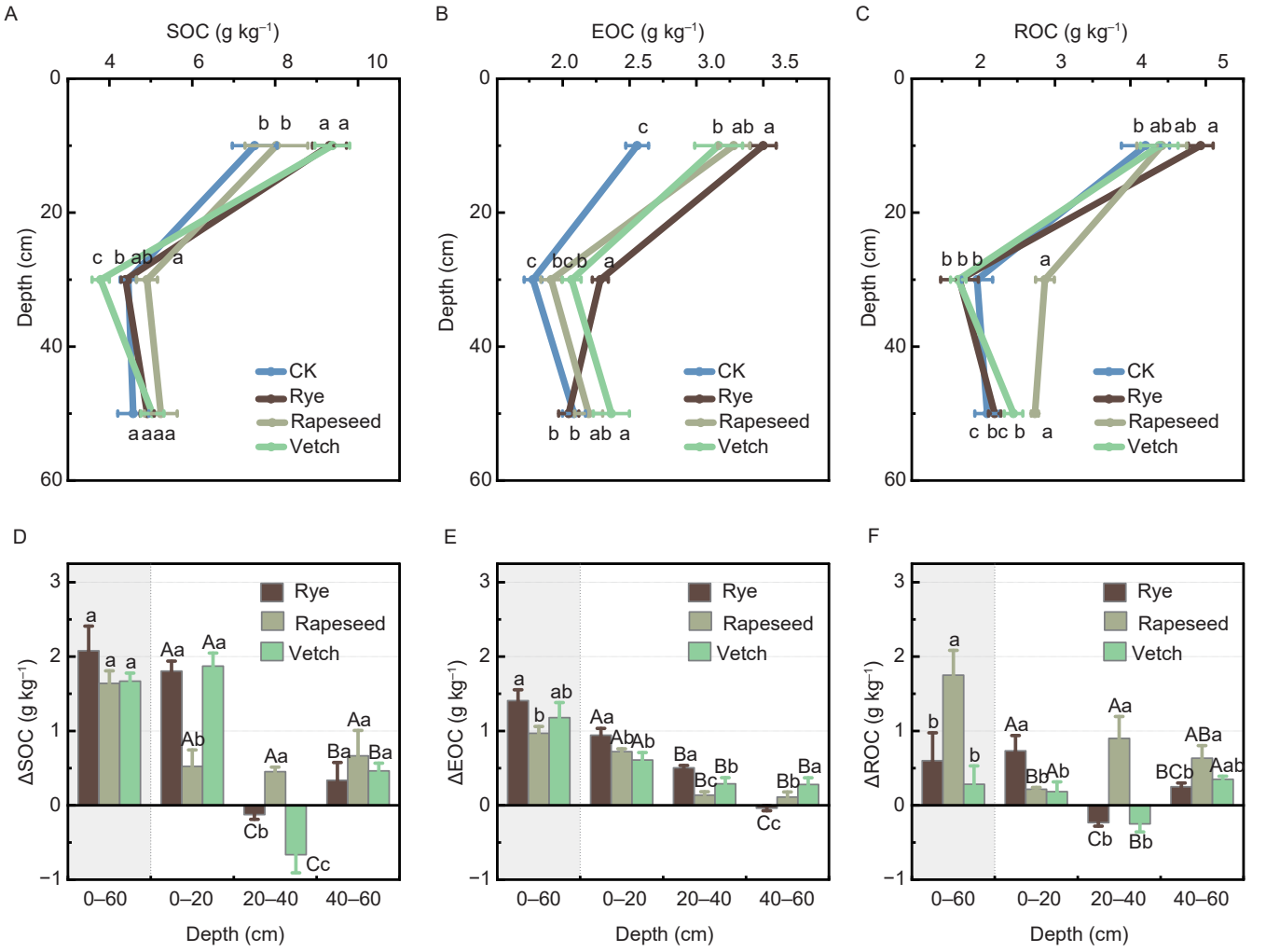


Fig. 2 Soil organic carbon (SOC; A), easily oxidizable carbon (EOC; B), recalcitrant organic carbon (ROC; C), and the change of SOC (ΔSOC; D), ECO (ΔEOC; E) and ROC (ΔROC; F) compared to CK across 0–60 cm soil profile. Error bar is SD (n=3). Different lowercase letters indicate significant differences among green manure treatments; different uppercase letters indicate significant differences among depths (P<0.05).

increase in ROC was also expressed across the 0–60 cm soil profile (P<0.05) (Fig. 2-F).

Furthermore, the CPMI for each GM treatment was calculated based on the proportion of EOC to SOC content (Appendix F). The CPMI patterns for rye and vetch treatments were similar, increasing from the 0–20 to 20–40 cm, and then decreasing from the 20–40 to 40–60 cm. Meanwhile, the CPMI for rapeseed treatment continuously decreased from the 0–60 cm (Fig. 3). The CPMI was significantly lower in the rapeseed treatment compared to rye and vetch treatments in the subsurface 20–60 cm soil.

3.3. Soil microbial C-decomposition functional genes

The absolute abundance of soil C-decomposition functional genes varied significantly among GM treatments (P<0.05), with notable declines for all genes from surface soil to subsurface soil (Appendix G). The $\log_2$(fold change) of genes, which compared gene abundance in GM treatments to the CK, showed that at the 0–20 cm, rye treatment significantly increased the abundance of *sga*, *abfA*, *chiA*, and *mpn* by $2^{1.5}$ to 2^4 folds (Fig. 4). These increases were significantly greater in rye than in rapeseed and vetch. Vetch primarily enhanced the abundance of *sga*, *cex*, *pgu*, and *mpn* at the 0–20 cm, with the highest $\log_2$(fold change) observed for *pgu*. In contrast, the $\log_2$ fold change for *sga*, *abfA*, and *chiA* in rapeseed were negative.

At the 20–40 cm, the $\log_2$(fold change) for *sga*, *abfA*, *chiA*, and *mpn* in rye remained higher, consistent with the pattern observed at the 0–20 cm. However, the $\log_2$(fold change) for *sga*, *abfA*, and *chiA* in rapeseed exhibited an opposite trend at this depth compared to the 0–20 cm. Meanwhile, the abundance of *sga* and *pgu* in vetch significantly decreased relative to the CK.

At the 40–60 cm depth, there were no significant changes in the abundance of *sga*, *abfA*, and *cex* across the GM treatments compared to the CK, and all GM treatments showed a modest increase in *pgu* and *mpn*. However, the abundance of *chiA* was significantly elevated only in the vetch treatment.

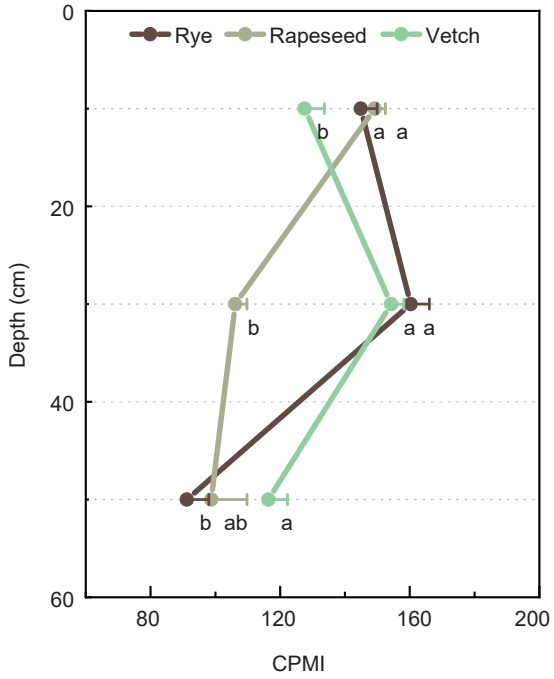


Fig. 3 Carbon pool management index (CPMI) across 0–60 cm soil profile under green manure treatments. Error bar is SD (n=3). Different lowercase letters indicate significant differences among green manure treatments (P<0.05).

3.4. Relationships among soil profile C fractions and C-decomposition functional genes

Redundancy analysis (RDA) was performed to investigate the relationship between C-decomposition genes and SOC fractions across different soil depths (Fig. 5). The RDA showed that the first component explained 90.34, 88.68, and 94.03% of the total variance at the 0–20, 20–40, and 40–60 cm, respectively. At the 0–20 cm, GM treatments were clearly separated from CK (Fig. 5-A). This separation was associated with the GM's C input, which was also positively correlated with all C-decomposition genes. Specifically, the gene abundances of *ITS*, *16S*, *mpn*, and *pgu* were responsible for the separation of vetch treatment, while *abfA*, *chiA* and *sga* were responsible for the separation of rye treatment. At the 20–40 cm, the rapeseed treatment was separated from CK, rye and vetch. The separation of rapeseed was driven by the increase of *pgu*, *mpn* and *cex* abundances (Fig. 5-B). At the 40–60 cm, rapeseed remained distinct from the CK and rye treatment, though other treatments overlapped more compared to 20–40 cm (Fig. 5-C). The separation at the 40–60 cm was less influenced by the GM's C input, while the separation of rapeseed was strongly associated with the abundances of *16S*, *sga*, *mpn*, *pgu* and *cex* abundances.

4. Discussion

4.1. Impact of green manure species on SOC depth distribution and recalcitrance

GM species differentially altered SOC across the soil profile, showing contrasting effects on SOC among soil depths (Fig. 2-D). When considering the 0–60 cm profile, SOC storage increased by 0.42–1.30 Mg ha^{-1} yr^{-1} under all the three GM species (Appendix H), aligning with previous research reporting an annual SOC storage increase of 0.32–1.75 Mg ha^{-1} yr^{-1} by GM (Poeplau and Don 2015; Zhang *et al.* 2019a). When considered by depth, the contrasting effects of GM species on SOC were evident in the vertical distribution of SOC, with rye and vetch primarily enhancing SOC at the 0–20 cm depth, whereas rapeseed significantly increased SOC at the 20–40 and 40–60 cm depths (Fig. 2-D). The greater SOC accumulation in the topsoil under rye and vetch could be attributed to enhanced C allocation to the surface layer. Specifically, this likely results from higher aboveground biomass C (Table 1) and shallow, fibrous and branched root systems of rye and vetch that concentrate C inputs near the surface (Materechera *et al.* 1992; Ren *et al.* 2022; Engedal *et al.* 2023). In contrast, subsurface SOC increase under rapeseed, particularly at 20–40 and 40–60 cm, was observed in this study and agreed with previous study (Wu *et al.* 2018). This SOC distribution under rapeseed can be explained by

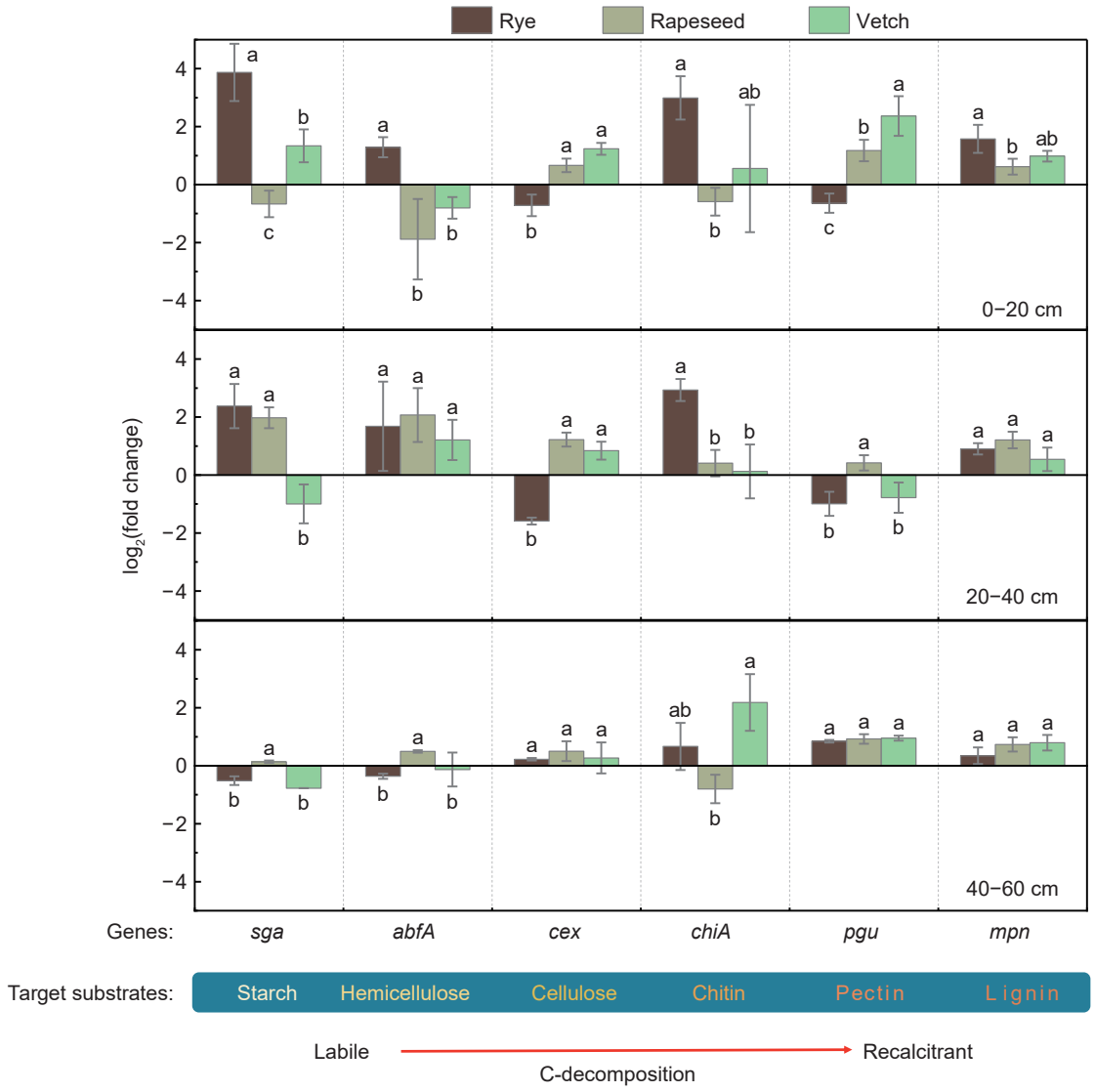


Fig. 4 log$_2$(fold change) of soil microbial C-decomposition functional genes between green manure treatments and the CK. Error bar is SD (n=3). Different lowercase letters indicate significant differences among green manure treatments (P<0.05).

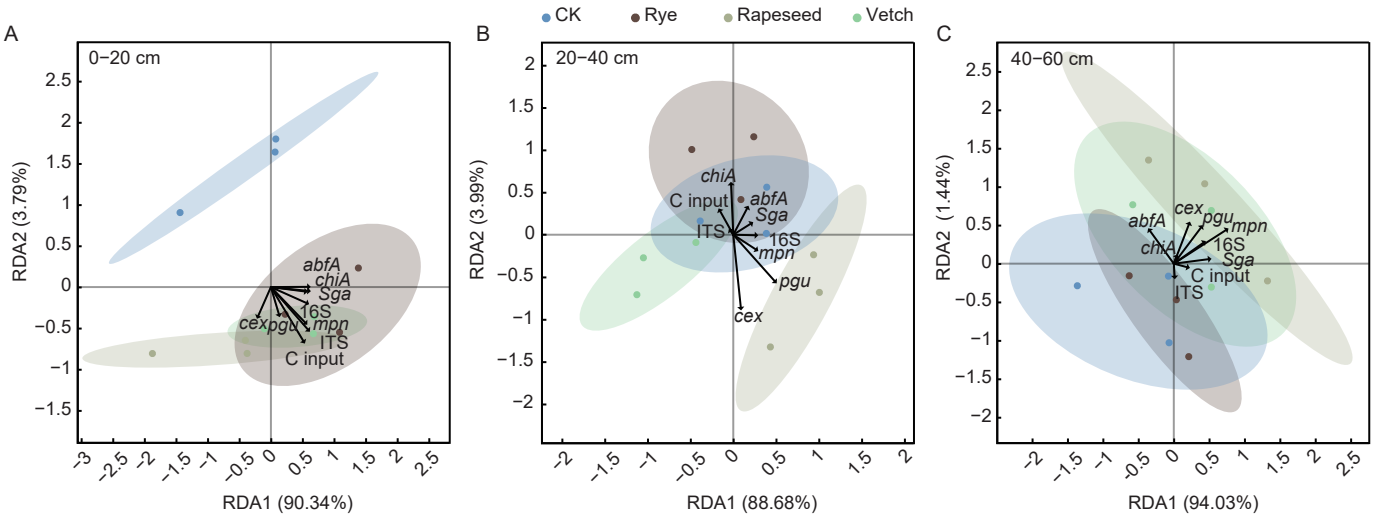


Fig. 5 Redundancy analyses (RDA) of relationships among soil C fractions and microbial C-decomposition functional genes at the 0–20 cm (A), 20–40 cm (B), 40–60 cm (C) depths.

its deep taproot system (Unkovich *et al.* 2023). Although root traits were not measured in this study, root morphology is known to influence the incorporation of rhizodeposition-derived C into SOC pools, where taproots promote SOC accumulation in deeper soil layers (Thorup-Kristensen *et al.* 2020; Engedal *et al.* 2023). Overall, the depth-specific SOC responses observed in this study highlight the role of growth-related differences among GM species in SOC sequestration.

GM species influenced not only the vertical distribution of SOC but also its recalcitrance (Fig. 2-E and F). Specifically, Rye enhanced both EOC and ROC in the topsoil, with a significant increase in ROC, likely due to rye's substantial C input with a high C:N ratio (Table 1). Such residues are relatively recalcitrant, slowing decomposition and enhanced ROC retention (Ruffo and Bollero 2003; Hoffland *et al.* 2020); consequently, ROC became the major component of SOC under rye in the topsoil (Appendix F).

In contrast to rye, vetch had the lowest biomass C:N ratio among the three GM species (Table 1) and significantly enhanced EOC in the subsoil, with the largest increase observed at 40–60 cm (Fig. 2-E). Its low C:N ratio biomass provided labile C input and decomposed rapidly, generating dissolved organic C that could be transported downward and accumulated as EOC in deeper soil layers (Tejada *et al.* 2008; Qiao *et al.* 2015). In addition, the taproot system of vetch, which branches extensively into both topsoil and subsoil (Materechera *et al.* 1992), likely contributed to C deposition in the subsurface and further replenished EOC in the subsoil. This observation is consistent with previous studies showing that branched roots with low C:N ratios can increase labile C in deeper soils (Nguyen 2003; Guo *et al.* 2004; Nguyen 2009; Xia *et al.* 2010).

Among the three GM species, rapeseed demonstrated a unique advantage in promoting SOC. Rapeseed was the only species that increased SOC content across all three soil layers, with the most significant increase in ROC at the 20–40 and 40–60 cm depths (Fig. 2-F). This could be attributed to rapeseed's superior root penetration ability, allowing it to penetrate compacted layers at 20–40 cm, where its lateral roots concentrated (Blanco-Canqui *et al.* 2015; Zhang W X *et al.* 2024). The accumulation of ROC under rapeseed suggests that its deep, rigid roots, capability of penetrating the plow pan, played a key role in depositing ROC in subsoil, driving SOC increase (Shi *et al.* 2023). Despite having lower C input compared to rye and vetch, rapeseed has better performance on enhancing 20–40 and 40–60 cm SOC storage.

To summarize the effects of GM species on SOC, we used the CPMI as an integrated indicator of changes in both SOC content and lability (Fig. 3). The markedly lower CPMI at 20–40 cm confirmed that rapeseed enhanced SOC storage mainly through the accumulation of recalcitrant organic C, whereas the substantial increase in CPMI at 40–60 cm under vetch indicated a greater capacity to improve C lability. Rye also exhibited a higher CPMI at 0–20 cm, which was primarily attributable to its large aboveground C input. The GM species influenced SOC content and recalcitrance, consistent with previous studies (Ma *et al.* 2018; Ni *et al.* 2021; Button *et al.* 2022), and our results further confirm that they shape the vertical distribution of SOC.

4.2. Efficiency of C conversion from GM biomass C into SOC

Three years of GM cultivation significantly increased the fraction of GM-derived C in SOC, as evidenced by the decline in soil $\delta^{13}C$ under GM crops (Fig. 1-B and C), and the efficiency of GM biomass C into SOC varied among GM species, confirmed our hypothesis that the conversion of GM biomass C into SOC is species-dependent.

It is noteworthy that rapeseed contributed the largest fraction of GM-derived C at 20–40 and 40–60 cm depths (Fig. 1-C), while it supplied the lowest above- and belowground biomass input (Table 1). The results from rapeseed contradict previous studies, which generally reported that the increase in GM-derived C was primarily induced by the high biomass C input of GMs (Qiao *et al.* 2015; Li *et al.* 2019, 2020; Ansari 2022). More GM-derived fraction in SOC under rapeseed than rye and vetch, indicating that less C underwent in microbial transformation (Chen *et al.* 2018; Zhang *et al.* 2022). This may be attributed to the higher content of recalcitrant materials in rapeseed input, such as lignin and other structural components that are more resistant to microbial decomposition (Guo *et al.* 2004; Bracey *et al.* 2022), as further evidenced by the higher ROC in the subsoil under rapeseed (Fig. 2-C).

Our results are consistent with previous studies showing that *Brassica* species such as rapeseed can deliver recalcitrant organic compounds into deeper soil layers through their taproot systems, thereby facilitating the accumulation of inert, oxidation-resistant organic C in the subsoil (Heinemann *et al.* 2023; Zhang S T *et al.* 2024). The 20–40 cm was the layer with the highest fraction of rapeseed-derived C incorporation (Fig. 1-C), and in the North China Plain it is typically the plough layer characterized by relatively high bulk density (Appendix E) and strong root penetration resistance (Shi *et al.* 2016). One possible explanation is that when the taproot of rapeseed penetrates the dense plough layer, it thickens and secretes abundant root exudates, which enhance C deposition at this depth (Guaman *et al.* 2016; Heinemann *et al.* 2023).

In summary, rapeseed with its taproot system exhibits higher C sequestration efficiency than fibrous-rooted species, particularly in 20–40 cm subsoils with greater bulk density and root penetration resistance. To verify the deep-soil C sequestration potential and underlying mechanisms of rapeseed, future studies would examine the biomass, thickness, and C composition of its roots, as well as conduct comparative analyses with other taproot GM species. Such efforts would provide stronger evidence for promoting rapeseed as a GM in the North China Plain.

4.3. C-decomposition genes influencing C transfer efficiency

Microbial C-decomposition genes also play a regulatory role in soil C decomposition, and their responses varied with GM species and soil depth. This was evidenced by the differential abundances of these genes (Fig. 4), and further supported by the RDA results showing the associations between SOC fractions and gene abundances (Fig. 5), confirming our

hypothesis that microbial C-decomposition genes regulate the transfer efficiency of plant-derived C into SOC.

Under rye, significantly higher abundances of C-degradation genes for *sga*, *abfA*, *chiA*, and *mpn* were observed at 0–20 cm (Fig. 4), occurring at the same depth as the high biomass C input. The surface C input and these genes aligned in RDA results and pointed the same direction in relation to SOC (Fig. 5-A), indicating that SOC incorporation under rye was jointly driven by biomass C input and microbial decomposition. These changes under rye are consistent with previous findings that C-decomposition genes facilitate the breakdown of plant biomass C and thereby improve SOC content (Gunina and Kuzyakov 2014; Ren *et al.* 2022).

Rapeseed enriched recalcitrant C-decomposition genes and SOC contents at the 20–40 cm depth (Fig. 4), combined with the RDA results showing that SOC fractions at this depth were primarily associated with *cex*, *pgu*, and *mpn* degradation genes (Fig. 5), suggesting that genes involved in recalcitrant-C such as pectin and lignin degradation are crucial drivers of SOC sequestration, which is also reported in recent studies (Hu *et al.* 2024; Li *et al.* 2024). Under rapeseed, the lowest C inputs nevertheless resulted in the highest SOC sequestration, indicating the greatest transfer efficiency and further confirming that recalcitrant-C pathways could be the primary mechanism contributing to SOC accumulation from rapeseed-derived C.

Vetch increased SOC content mainly at 0–20 and 40–60 cm depths. At 0–20 cm, the dominant C-decomposition genes were related to *sga*, *cex*, *pgu*, and *mpn* (Fig. 4). Combined with the RDA results, this indicates that the factors affecting SOC at 0–20 cm under vetch were similar to those under rye, suggesting that SOC incorporation in the topsoil was jointly regulated by C inputs and C-decomposition genes (Fig. 5-A). The genes recruited in topsoil could be generally due to the large input of labile substrates such as starch and cellulose, as well as by the low C/N ratio of legume biomass that facilitates decomposition (Dong *et al.* 2024). Such labile inputs have been reported to stimulate microbial activity and accelerate the breakdown of structural compounds like lignin (Moorhead and Sinsabaugh 2006; Franke *et al.* 2008; Talbot and Treseder 2012; He *et al.* 2019; Zhang *et al.* 2019b), which may also explain the increase of *mpn* associated gene. On the other hand, at 40–60 cm, the major enriched genes were related to *chiA*, *pgu*, and *mpn* (Fig. 4). The C-decomposition pathways in the deep soil showed greater similarity to those under rapeseed, suggesting that SOC incorporation at this depth was predominantly controlled by recalcitrant C-decomposition genes.

In this study, microbial decomposition specialization also aligns with SOC recalcitrance. Such microbial specialization facilitated the selective preservation and accumulation of recalcitrant C (Li *et al.* 2023). In summary, these findings highlight that the microbial C-decomposition functional genes under GM crops mediate both the efficiency and stability of SOC incorporation, and their effects are depth-dependent. Future research should employ metagenomic approaches to further dissect how specific microbial community structures and metabolic pathways regulate SOC stabilization across different soil depths.

5. Conclusion

This three-year study on the North China Plain demonstrated that incorporating GM during winter fallow significantly enhanced SOC across the 0–60 cm profile, with species-specific effects on depth distribution and SOC stability. Rye and vetch increased EOC and ROC mainly in the topsoil, while rapeseed uniquely promoted ROC accumulation in the 20–40 and 40–60 cm subsoil despite lower biomass inputs. These contrasting outcomes indicate that SOC sequestration under different GM species is regulated not only by the quantity of biomass, but also by the combined influence of biomass quality, depth of C deposition, and microbial decomposition specialization, which together determine the efficiency and stability of SOC storage. Accordingly, selecting GM species based on their sequestration characteristics and targeted soil layers provides a practical strategy to achieve desired outcomes: either enhancing short-term C availability or promoting long-term SOC stability.

Acknowledgements

The work was partly funded by the National Key Research and Development Program of China (2021YFD1700204-02), the National Natural Science Foundation of China (42077099), the Earmarked Fund of the China Agriculture Research System (CARS-04), and the Agricultural Science and Technology Innovation Program of Chinese Academy Agricultural Sciences (ASTIP-G2024–01–06).

Declaration of competing interest

The authors declare that they have no conflict of interest.

Declaration of generative AI and AI-assisted technologies in the writing process

During the preparation of this manuscript, the authors used ChatGPT 4.5 to assist in improving the clarity and readability of the language. All content generated was carefully reviewed and revised by the authors as necessary, and the authors take full responsibility for the final content of the article.

Appendices associated with this paper are available at https://doi.org/10.1016/j.jia.2025.11.005

References

Ansari M A, Choudhury B U, Layek J, Das A, Lal R, Mishra V K. 2022. Green manuring and crop residue management: Effect on soil organic carbon stock, aggregation, and system productivity in the foothills of Eastern Himalaya (India). *Soil and Tillage Research*, **218**, 105318.

Balesdent J, Mariotti A, Guillet B. 1987. Natural ^{13}C abundance as a tracer for studies of soil organic matter dynamics. *Soil Biology and Biochemistry*, **19**, 25–30.

Berendsen R L, Pieterse C M J, Bakker P A H M. 2012. The rhizosphere microbiome and plant health. *Trends in Plant Science*, **17**, 478–486.

Blair G J, Lefroy R D, Lisle L. 1995. Soil carbon fractions based on their degree of oxidation, and the development of a carbon management index for agricultural systems. *Australian Journal of Agricultural Research*, **46**, 1459–1466.

Blanco-Canqui H, Shaver T M, Lindquist J L, Shapiro C A, Elmore R W, Francis C A, Hergert G W. 2015. Cover crops and ecosystem

services: insights from studies in temperate soils. *Agronomy Journal*, **107**, 2449–2474.
Bracey W M, Sykes V R, Yin X H, Bates G E, Butler D M, McIntosh D W, Willette A R. 2022. Forage yield, quality, and impact on subsequent cash crop of cover crops in an integrated forage/row crop system. *Agronomy*, **12**, 1214.
Busari M A, Salako F K, Tuniz C. 2016. Stable isotope technique in the evaluation of tillage and fertilizer effects on soil carbon and nitrogen sequestration and water use efficiency. *European Journal of Agronomy*, **73**, 98–106.
Button E S, Pett-Ridge J, Murphy D V, Kuzyakov Y, Chadwick D R, Jones D L. 2022. Deep-C storage: Biological, chemical and physical strategies to enhance carbon stocks in agricultural subsoils. *Soil Biology and Biochemistry*, **170**, 108697.
Chen J, Heiling M, Resch C, Mbaye M, Gruber R, Dercon G. 2018. Does maize and legume crop residue mulch matter in soil organic carbon sequestration? *Agriculture*, *Ecosystems & Environment*, **265**, 123–131.
Chen L Y, Liu L, Qin S Q, Yang G B, Fang K, Zhu B, Kuzyakov Y, Chen P D, Xu Y P, Yang Y H. 2019. Regulation of priming effect by soil organic matter stability over a broad geographic scale. *Nature Communications*, **10**, 5112.
Chen Y L, Zhang Y H, Li C, Xu R S, Pei Z R, Li F C, Wu Y H, Chen F, Liang Y R, Li Z H, Tian X H, Wang Y H. 2023. Linking soil organic carbon dynamics to microbial community and enzyme activities in degraded soil remediation by reductive soil disinfestation. *Applied Soil Ecology*, **189**, 104931.
Cotrufo M F, Lavallee J M. 2022. Soil organic matter formation, persistence, and functioning: A synthesis of current understanding to inform its conservation and regeneration. *Advances in Agronomy*, **172**, 1–66.
Dong R S, Hu W, Bu L Y, Cheng H T, Liu G D. 2024. Legume cover crops alter soil phosphorus availability and microbial community composition in mango orchards in karst areas. *Agriculture*, *Ecosystems & Environment*, **364**, 108906.
Dou X L, Cheng X L, He P, Zhu P, Zhou W, Wang L G. 2017. Dynamics of physically-separated soil organic carbon pools assessed from δ^{13}C changes under 25 years of cropping systems. *Soil and Tillage Research*, **174**, 6–13.
Engedal T, Magid J, Hansen V, Rasmussen J, Sørensen H, Jensen L S. 2023. Cover crop root morphology rather than quality controls the fate of root and rhizodeposition C into distinct soil C pools. *Global Change Biology*, **29**, 5677–5690.
Franke A C, Laberge G, Oyewole B D, Schulz S. 2008. A comparison between legume technologies and fallow, and their effects on maize and soil traits, in two distinct environments of the West African savannah. *Nutrient Cycling Agroecosystems*, **82**, 117–135.
Gao S J, Li S, Zhou G P, Cao W D. 2023. The potential of green manure to increase soil carbon sequestration and reduce the yield-scaled carbon footprint of rice production in southern China. *Journal of Integrative Agriculture*, **22**, 2233–2247.
Griscom B W, Adams J, Ellis P W, Houghton R A, Lomax G, Miteva D A, Schlesinger W H, Shoch D, Siikamäki J V, Smith P, Woodbury P, Zganjar C, Blackman A, Campari J, Conant R T, Delgado C, Elias P, Gopalakrishna T, Hamsik M R, Herrero M, *et al.* 2017. Natural climate solutions. *Proceedings of the National Academy of Sciences of the United States of America*, **114**, 11645–11650.
Guaman V, Båth B, Hagman J, Gunnarsson A, Persson P. 2016. Short time effects of biological and inter-row subsoiling on yield of potatoes grown on a loamy sand, and on soil penetration resistance, root growth and nitrogen uptake. *European Journal of Agronomy*, **80**, 55–65.
Gunina A, Kuzyakov Y. 2014. Pathways of litter C by formation of aggregates and SOM density fractions: Implications from ^{13}C natural abundance. *Soil Biology and Biochemistry*, **71**, 95–104.
Guo D L, Mitchell R J, Hendricks J J. 2004. Fine root branch orders respond differentially to carbon source-sink manipulations in a longleaf pine forest. *Oecologia*, **140**, 450–457.
Haynes R J. 2000. Labile organic matter as an indicator of organic matter quality in arable and pastoral soils in New Zealand. *Soil Biology and Biochemistry*, **32**, 211–219.
He H B, Li W X, Zhang Y W, Cheng J K, Jia X Y, Li S, Yang H R, Chen B M, Xin G R. 2020. Effects of Italian ryegrass residues as green manure on soil properties and bacterial communities under an Italian ryegrass (*Lolium multiflorum* L.)–rice (*Oryza sativa* L.) rotation. *Soil and Tillage Research*, **196**, 104487.
He M, Zhao R D, Tian Q X, Huang L, Wang X G, Liu F. 2019. Predominant effects of litter chemistry on lignin degradation in the early stage of leaf litter decomposition. *Plant and Soil*, **442**, 453–469.
Heinemann H, Hirte J, Seidel F, Don A. 2023. Increasing root biomass derived carbon input to agricultural soils by genotype selection — a review. *Plant and Soil*, **490**, 19–30.
Hoffland E, Kuyper T W, Comans R N J, Creamer R E. 2020. Eco-functionality of organic matter in soils. *Plant and Soil*, **455**, 1–22.
Hu Q J, Zhang Y T, Cao W D, Yang Y Y, Hu Y X, He T G, Li Z Y, Wang P, Chen X P, Chen J, Shi X J. 2024. Legume cover crops sequester more soil organic carbon than non-legume cover crops by stimulating microbial transformations. *Geoderma*, **450**, 117024.
Huang W G, Kuzyakov Y, Niu S L, Luo Y, Sun B, Zhang J B, Liang Y T. 2023. Drivers of microbially and plant-derived carbon in topsoil and subsoil. *Global Change Biology*, **29**, 6188–6200.
IPCC (The Intergovernmental Panel on Climate Change). 2018. Technical summary: In special report on global warming of 1.5°C. [2024-9-24]. https://www.ipcc.ch/sr15/resources/technicalsummary/
Kumar S, Meena R S, Lal R, Yadav G S, Mitran T, Meena B L, Dotaniya M L, EL-Sabagh A. 2018. Role of legumes in soil carbon sequestration. In: Meena R S, Das A, Yadav G S, Lal R, eds., *Legumes for Soil Health and Sustainable Management*. Springer, Singapore. pp. 109–138.
Leue M, Uteau D, Peth S, Beck-Broichsitter S, Gerke H H. 2020. Volume-related quantification of organic carbon content and cation exchange capacity of macropore surfaces in Bt horizons. *Vadose Zone Journal*, **19**, e20069.
Li H T, Fan Z L, Hu F L, Yin W, Wang Q M, Wang G C, Cao W D, He W, Chai Q, Yao T. 2025. Intercropping maize with leguminous green manure can compensate for the losses in grain yield and N uptake caused by a reduced N supply. *Journal of Integrative Agriculture*, **24**, 2826–2840.
Li P, Jia L, Chen Q Q, Zhang H J, Deng J J, Lu J Y, Xu L, Li H X, Hu F, Jiao J G. 2024. Adaptive evaluation for agricultural sustainability of different fertilizer management options for a green manure–maize rotation system: Impacts on crop yield, soil biochemical properties and organic carbon fractions. *Science of the Total Environment*, **908**, 168170.
Li T, Gao J S, Bai L Y, Wang Y N, Huang J, Kumar M, Zeng X B. 2019. Influence of green manure and rice straw management on soil organic carbon, enzyme activities, and rice yield in red paddy soil. *Soil and Tillage Research*, **195**, 104428.
Li Y, Zhang W, Li J, Zhou F, Liang X N, Zhu X F, He H B, Zhang X D. 2023. Complementation between microbial necromass and plant debris governs the long-term build-up of the soil organic carbon pool in conservation agriculture. *Soil Biology and Biochemistry*, **178**, 108963.
Li Z Q, Zhang X, Xu J, Cao K, Wang J H, Xu C X, Cao W D. 2020. Green manure incorporation with reductions in chemical fertilizer inputs improves rice yield and soil organic matter accumulation. *Journal of Soils and Sediments*, **20**, 2784–2793.
Liu B, Xia H, Jiang C C, Riaz M, Yang L, Chen Y F, Fan X P, Xia X G. 2022. 14 year applications of chemical fertilizers and crop straw effects on soil labile organic carbon fractions, enzyme activities and microbial community in rice–wheat rotation of middle China. *Science of the Total Environment*, **841**, 156608.
Liu Q, Yao W, Zhou J, Peixoto L, Qi Z Q, Mganga K Z, Yang Y D, Zeng Z H, Zang H D. 2024. Winter green manure cultivation benefits soil quality and ecosystem multifunctionality under upland paddy rotations in tropics. *Plant and Soil*, **511**, 395–407.
Ma D K, Yin L N, Ju W L, Li X K, Liu X X, Deng X P, Wang S W. 2021. Meta-analysis of green manure effects on soil properties and crop yield in northern China. *Field Crops Research*, **266**, 108146.
Ma T, Zhu S S, Wang Z H, Chen D M, Dai G H, Feng B W, Su X Y, Hu H F, Li K H, Han W X, Liang C, Bai Y F, Feng X J. 2018. Divergent accumulation of microbial necromass and plant lignin components in grassland soils. *Nature Communications*, **9**, 3480.
Magdoff F, Weil R R. 2004. Significance of soil organic matter to soil quality and health. In: Magdoff F, Weil R R, eds., *Soil Organic Matter in Sustainable Agriculture*. Chemical & Rubber & Company Press, New York. pp. 1–43.
Materechera S A, Alston A M, Kirby J M, Dexter A R. 1992. Influence of root diameter on the penetration of seminal roots into a compacted

subsoil. *Plant and Soil*, **144**, 297–303.
Moorhead D L, Sinsabaugh R L. 2006. A theoretical model of litter decay and microbial interaction. *Ecological Monographs*, **76**, 151–174.
Nguyen C. 2003. Rhizodeposition of organic C by plants: Mechanisms and controls. *Agronomie*, **23**, 375–396.
Nguyen C. 2009. Rhizodeposition of organic C by plant: Mechanisms and controls. In: Lichtfouse E, Navarrete M, Debaeke P, Véronique S, Alberola C, eds., *Sustainable Agriculture*. Springer Netherlands, Dordrecht. pp. 97–123.
Ni H W, Jing X Y, Xiao X, Zhang N, Wang X Y, Sui Y Y, Sun B, Liang Y T. 2021. Microbial metabolism and necromass mediated fertilization effect on soil organic carbon after long-term community incubation in different climates. *The ISME Journal*, **15**, 2561–2573.
Nouri A, Lee J, Yin X H, Tyler D D, Saxton A M. 2019. Thirty-four years of no-tillage and cover crops improve soil quality and increase cotton yield in Alfisols, Southeastern USA. *Geoderma*, **337**, 998–1008.
Poeplau C, Don A. 2015. Carbon sequestration in agricultural soils via cultivation of cover crops — A meta-analysis. *Agriculture, Ecosystems & Environment*, **200**, 33–41.
Qiao Y F, Miao S J, Li N, Xu Y L, Han X Z, Zhang B. 2015. Crop species affect soil organic carbon turnover in soil profile and among aggregate sizes in a Mollisol as estimated from natural ^{13}C abundance. *Plant and Soil*, **392**, 163–174.
Ramírez P B, Fuentes-Alburquenque S, Díez B, Vargas I, Bonilla C A. 2020. Soil microbial community responses to labile organic carbon fractions in relation to soil type and land use along a climate gradient. *Soil Biology and Biochemistry*, **141**, 107692.
Regnier P, Friedlingstein P, Ciais P, Mackenzie F T, Gruber N, Janssens I A, Laruelle G G, Lauerwald R, Luyssaert S, Andersson A J, Arndt S, Arnosti C, Borges A V, Dale A W, Gallego-Sala A, Goddéris Y, Goossens N, Hartmann J, Heinze C, Ilyina T, *et al.* 2013. Anthropogenic perturbation of the carbon fluxes from land to ocean. *Nature Geoscience*, **6**, 597–607.
Ren L D, Cornelis W M, Ruysschaert G, De Pue J, Lootens P, D'Hose T. 2022. Quantifying the impact of induced topsoil and historical subsoil compaction as well as the persistence of subsoiling. *Geoderma*, **424**, 116024.
Rocci K S, Lavallee J M, Stewart C E, Cotrufo M F. 2021. Soil organic carbon response to global environmental change depends on its distribution between mineral-associated and particulate organic matter: A meta-analysis. *Science of the Total Environment*, **793**, 148569.
de Rouw A, Soulileuth B, Huon S. 2015. Stable carbon isotope ratios in soil and vegetation shift with cultivation practices (Northern Laos). *Agriculture, Ecosystems & Environment*, **200**, 161–168.
Rovira P, Vallejo V R. 2007. Labile, recalcitrant, and inert organic matter in Mediterranean forest soils. *Soil Biology and Biochemistry*, **39**, 202–215.
Ruffo M L, Bollero G A. 2003. Modeling Rye and hairy vetch residue decomposition as a function of degree-days and decomposition-days. *Agronomy Journal*, **95**, 900–907.
Shi J W, Song M Y, Yang L, Zhao F, Wu J Z, Li J W, Yu Z J, Li A, Shangguan Z P, Deng L. 2023. Recalcitrant organic carbon plays a key role in soil carbon sequestration along a long-term vegetation succession on the Loess Plateau. *Catena*, **233**, 107528.
Shi Y, Yu Z W, Man J G, Ma S Y, Gao Z Q, Zhang Y L. 2016. Tillage practices affect dry matter accumulation and grain yield in winter wheat in the North China Plain. *Soil and Tillage Research*, **160**, 73–81.
Talbot J M, Treseder K K. 2012. Interactions among lignin, cellulose, and nitrogen drive litter chemistry–decay relationships. *Ecology*, **93**, 345–354.
Tejada M, Gonzalez J L, García-Martínez A M , Parrado J. 2008. Effects of different green manures on soil biological properties and maize yield. *Bioresource Technology*, **99**, 1758–1767.
Thorup-Kristensen K, Halberg N, Nicolaisen M, Olesen J E, Crews T E, Hinsinger P, Kirkegaard J, Pierret A, Dresbøll D B. 2020. Digging deeper for agricultural resources, the value of deep rooting. *Trends in Plant Science*, **25**, 406–417.
Tian H Q, Lu C Q, Yang J, Banger K, Huntzinger D N, Schwalm C R, Michalak A M, Cook R, Ciais P, Hayes D, Huang M Y, Ito A, Jain A K, Lei H M, Mao J F, Pan S F, Post W M, Peng S S, Poulter B, Ren W, *et al.* 2015. Global patterns and controls of soil organic carbon dynamics as simulated by multiple terrestrial biosphere models: Current status and future directions. *Global Biogeochemical Cycles*, **29**, 775–792.
Unkovich M, McKenzie D, Parker W. 2023. New insights into high soil strength and crop plants; implications for grain crop production in the Australian environment. *Plant and Soil*, **486**, 183–208.
Wang B, Huang X H, Chen J F, Fu L B, Chen Y Q, Gao W S, Sui P. 2024. Intercropping with green manure regulates microbial community structure and improves tea quality by changing soil available nutrients under organic management. *Land Degradation & Development*, **36**, 1384–1397.
Wang X, Wang C, Cotrufo M F, Sun L F, Jiang P, Liu Z P, Bai E. 2020. Elevated temperature increases the accumulation of microbial necromass nitrogen in soil via increasing microbial turnover. *Global Change Biology*, **26**, 5277–5289.
Wang X, Zhu X M, Fang Y Y, Vancov T, Zou Z C, Jin X Y, Ma L X, Wu D, Du Z L. 2025. Long-term nitrogen fertilization accelerates labile biomolecules decomposition and retains recalcitrant compounds in a temperate agroecosystem. *Agriculture, Ecosystems & Environment*, **379**, 109373.
Wu H W, Li J, Zhang C C, He B, Zhang H X, Wu X C, Li X Y. 2018. Determining root water uptake of two alpine crops in a rainfed cropland in the Qinghai Lake watershed: First assessment using stable isotopes analysis. *Field Crops Research*, **215**, 113–121.
Xia M X, Guo D L, Pregitzer K S. 2010. Ephemeral root modules in Fraxinus mandshurica. *New Phytologist*, **188**, 1065–1074.
Xia S P, Song Z L, Van Zwieten L, Guo L D, Yu C X, Wang W Q, Li Q, Hartley I P, Yang Y H, Liu H Y, Wang Y D, Ran X B, Liu C Q, Wang H L. 2022. Storage, patterns and influencing factors for soil organic carbon in coastal wetlands of China. *Global Change Biology*, **28**, 6065–6085.
Xiang H M, Luo X Z, Zhang L L, Hou E Q, Li J, Zhu Q D, Wen D Z. 2022. Forest succession accelerates soil carbon accumulation by increasing recalcitrant carbon stock in subtropical forest topsoils. *Catena*, **212**, 106030.
Yan Z J, Zhou J, Liu C Y, Jia R, Mganga K Z, Yang L, Yang Y D, Peixoto L, Zang H D, Zeng Z H. 2023. Legume-based crop diversification reinforces soil health and carbon storage driven by microbial biomass and aggregates. *Soil and Tillage Research*, **234**, 105848.
Zechmeister-Boltenstern S, Keiblinger K M, Mooshammer M, Peñuelas J, Richter A, Sardans J, Wanek W. 2015. The application of ecological stoichiometry to plant–microbial–soil organic matter transformations. *Ecological Monographs*, **85**, 133–155.
Zhang D B, Yao P W, Zhao N, Cao W D, Zhang S Q, Li Y Y, Huang D L, Zhai B N, Wang Z H, Gao Y J. 2019a. Building up the soil carbon pool via the cultivation of green manure crops in the Loess Plateau of China. *Geoderma*, **337**, 425–433.
Zhang D B, Yao Z Y, Chen J, Yao P W, Zhao N, He W X, Li Y Y, Zhang S Q, Zhai B N, Wang Z H, Huang D L, Cao W D, Gao Y J. 2019b. Improving soil aggregation, aggregate-associated C and N, and enzyme activities by green manure crops in the Loess Plateau of China. *European Journal of Soil Science*, **70**, 1267–1279.
Zhang J, Kuang L H, Mou Z J, Kondo T, Koarashi J, Atarashi-Andoh M, Li Y, Tang X L, Wang Y P, Peñuelas J, Sardans J, Hui D F, Lambers H, Wu W J, Kaal J, Li J, Liang N S, Liu Z F. 2022. Ten years of warming increased plant-derived carbon accumulation in an East Asian monsoon forest. *Plant and Soil*, **481**, 349–365.
Zhang S T, Ren T, Cong W F, Fang Y T, Zhu J, Zhao J, Cong R H, Li X K, Lu J W. 2024. Oilseed rape-rice rotation with recommended fertilization and straw returning enhances soil organic carbon sequestration through influencing macroaggregates and molecular complexity. *Agriculture, Ecosystems & Environment*, **367**, 108960.
Zhang W X, Wu Q, Sun C L, Ge D K, Cao J, Liang W J, Yin Y J, Li H, Cao H X, Zhang W Y, Li B M, Xin Y K. 2024. Biomass-based lateral root morphological parameter models for rapeseed (*Brassica napus* L.). *Food and Energy Security*, **13**, e519.

Executive Editor-in-Chief Jinshui Wu
Managing Editor Lujuan Sun